Rock and Soil Mechanics

Volume 42 | Issue 11 Article 4

2-23-2022

The effect of initial water content on the consolidation of dredged slurry under vacuum preloading

Hong-lei SUN
College of Civil Engineering, Zhejiang University of Technology, Hangzhou, Zhejiang 310014, China

Yi LU
Hangzhou Tianyuan Architectural Design & Research Institute Co., Ltd, Hangzhou, Zhejiang 311202, China

Xiao-dong PAN
College of Civil Engineering, Zhejiang University of Technology, Hangzhou, Zhejiang 310014, China

Li SHI
College of Civil Engineering, Zhejiang University of Technology, Hangzhou, Zhejiang 310014, China

See next page for additional authors

Custom Citation

SUN Hong-lei, LU Yi, PAN Xiao-dong, SHI Li, CAI Yuan-qiang, . The effect of initial water content on the consolidation of dredged slurry under vacuum preloading[J]. Rock and Soil Mechanics, 2021, 42(11): 3029-3040.

The effect of initial water content on the consolidation of dredged slurry under vacuum preloading

Authors

Hong-lei SUN, Yi LU, Xiao-dong PAN, Li SHI, and Yuan-qiang CAI

Rock and Soil Mechanics 2021 42(11): 3029−3040 ISSN 1000−7598
https: //doi.org/10.16285/j.rsm.2021.5180 rocksoilmech.researchcommons.org/journal

The effect of initial water content on the consolidation of dredged slurry under vacuum preloading

SUN Hong-lei[1], LU Yi[2], PAN Xiao-dong[1], SHI Li[1], CAI Yuan-qiang[1]
1. College of Civil Engineering, Zhejiang University of Technology, Hangzhou, Zhejiang 310014, China
2. Hangzhou Tianyuan Architectural Design & Research Institute Co., Ltd, Hangzhou, Zhejiang 311202, China

Abstract: In the process of treating the dredged slurry under vacuum preloading combined with the prefabricated vertical drains (PVDs), a dense "soil column" with low permeability will be formed around the PVD, which results in a poor drainage condition and an unsatisfactory treatment (i.e., the clogging effect). In this study, in order to predict the consolidation behavior of dredged slurry with different initial water contents, the compressibility and permeability of dredged slurry with different initial water contents are investigated. Based on the compression and permeability curves obtained by laboratory tests, the analytical solution to soil consolidation under vacuum preloading is derived. Both the clogging effect and the effect of the initial water content on the initial effective stress are considered. The developed analytical solution is validated through a series of consolidation tests of dredged slurry under vacuum preloading with different initial water contents. It shows that at a given vacuum preloading, the dissipation rate of excess pore water pressure in the dredged slurry decreases as the initial water content increases. The proposed analytical solution presents reliable predictions on the variation of settlement and degree of consolidation with time in the dredged slurry with different initial water contents under vacuum preloading.

Keywords: vacuum preloading; dredged slurry; initial water content; consolidation theory; settlement prediction

1 Introduction

The dredged slurries contain high water contents and behave as a fluid, which are extremely unfavorable in engineering practice. Thus, the dredged slurries need to be treated to satisfy the requirements for further utilization[1−4]. A vacuum preloading combined with prefabricated vertical drain (PVD) is widely used for ground improvement with dredged slurries with high initial water contents, which is economical and eco-friendly[5−9]. An obconical dense soil zone, i.e., "soil column", gradually forms surrounding the PVD during the consolidation of dredged slurries under vacuum preloading. The "soil column" usually has a lower permeability, which results in poor drainage and incomplete consolidation conditions. However, these problems do not appear in the process of this technology to treat natural sediment foundations with low initial moisture content. Therefore, numerous studies have been conducted to investigate the phenomenon by model tests and theoretical analysis.

Shen[11] conducted the laboratory model tests on dredged slurries under traditional vacuum preloading with different soil types and initial water contents. The test results indicated that the initial water content greatly influenced the consolidation behavior. The dredged slurry with a lower initial water content gained a higher strength after the ground improvement by the vacuum preloading. Yan and Chu[12] performed a case study for treating the dredged slurry foundation of a port in Tianjin, China, using the combined vacuum and surcharge preloading method. They concluded that the high initial water content and the low initial strength of dredged slurry resulted in inadequate consolidation. Lou[13] conducted laboratory model tests to investigate the effects of vertical drains and the initial water content on the consolidation of slurries under vacuum preloading and concluded that the strength of dredged slurries after the completion of consolidation would decrease linearly as the initial water content increases. Deng et al.[14] carried out a series of vacuum preloading model tests with tidal mud. The results showed that the transmission of vacuum load in tidal mud with high moisture content would be seriously hindered, resulting in limited reinforcement range and uneven reinforcement effect. Wang et al.[15] and Han[16] conducted the laboratory model tests on three different soils and found a similar clogging effect of the "soil column" that compromised the improvement quality. They studied the effect of the non-uniform consolidation on the degree of consolidation and proposed a method for evaluating the average radial coefficient of consolidation. Tai et al.[17] used gabion as the research object to explore the causes of soil clogging using the computed tomography (CT) scanning technique. The higher the initial water content of the soil sample, the severer the clogging effect, which was identified by the CT scanning results because the pore size of the PVD filter is much smaller than that of the gabion. Based on the findings, they proposed a mathematical consolidation model considering the time-dependent clogging effect. In summary, the initial water content significantly influences the reinforcement effect under vacuum preloading for dredged soils. The initial water content is a key factor that should be considered in the experimental studies on the consolidation

Received: 13 May 2021 Revised: 24 September 2021
The work was supported by the National Natural Science Foundation of China (52078464, 51879234, 51978621, 51620105008), the National Key R&D Program of China (2016YFC0800200) and the Key R&D Program of Zhejiang Province (2018C03038).
First author: SUN Hong-lei, male, born in 1981, PhD, Professor, mainly engaged in research on geotechnical engineering. E-mail: sunhonglei@zju.edu.cn

of dredged slurries. The existing predictive models usually underestimate or overestimate the degree of consolidation of dredged slurry ground with high initial water content and high compressibility. To the best of the authors' knowledge, the analytical models for predicting the consolidation behavior of dredged slurries under vacuum preloading considering different initial water contents have not been proposed in the literature. Thus, the experimental studies and analytical analysis directed to this aspect will be conducted in this study.

To investigate the effect of the initial water content on the consolidation behavior of dredged slurries, the modified oedometer tests with a low initial stress and laboratory permeability tests were conducted in this study. Based on the laboratory test results, the effects of "soil column" and initial water content on compressibility and permeability were considered in the analytical model development to propose an analytical solution of dredged slurries under vacuum preloading that reflects the variation of compressibility and permeability coefficient with different initial water content. The vacuum preloading model tests with different initial moisture content were carried out, and the comparison and agreement between the predictions by the proposed model and the measurements validated the proposed analytical model in this study.

2 Effect of water content on soil compressibility and permeability

A vacuum preloading combined with PVD is used to treat and strengthen the dredged slurry with high initial water content. To evaluate the consolidation characteristics of the dredged slurry ground after consolidation, detailed information on the real soil properties is required, such as deformation parameters (compressibility), permeability coefficient, consolidation parameters, and others[4]. The compressibility and permeability have a remarkable influence on the consolidation behavior of the soil under vacuum preloading, which are typically obtained by laboratory experiments, in-situ tests, and back-analysis based on field data. The laboratory experiments, such as the oedometer test and the permeability test, are the most commonly used approaches to determine the compressibility and permeability of the soil. The variation of the void ratio with the vertical effective stress can be obtained by interpreting the consolidation test results to calculate the coefficients of compression and consolidation[9]. The permeability coefficients at various states can be determined by the permeability test.

2.1 Soil properties

The soil samples used in this study were collected from Taizhou, Zhejiang Province, China. Following the *Standard for Geotechnical Testing Method* (GB/T 50123 — 2019)[18], laboratory experiments on the fundamental physical properties of the soil sample were conducted, and the test results are shown in Table 1. The liquid limit and plastic limit of the soil samples are 40% and 23%, respectively. The particle size distribution of the soil sample was determined by the densimeter method, which is presented on a semi-logarithmic plot, as shown in Fig. 1. The soil sample mainly consists of silt size fraction (0.005–0.075 mm) and clay size fraction (< 0.005 mm), which are 55.0% and 13.5% of the total sample by weight. The soil sample is clay with a low liquid limit (CL) according to the *Standard for Geotechnical Testing Method* (GB/T 50123—2019)[18].

Table 1 Basic physical properties of soil sample

Specific gravity G_s	Natural water content w_0 /%	Liquid limit w_L /%	Plastic limit w_P /%	Median particle size d_{50} /μm
2.674	78	40	23	20.148

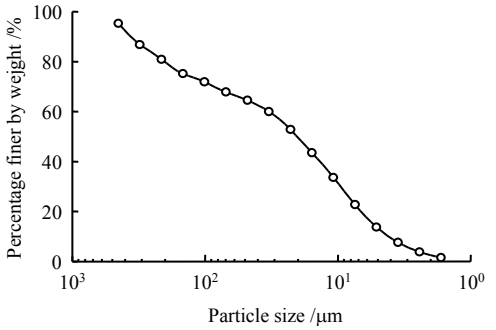

Fig. 1 Particle size distribution curve of soil sample

2.2 Effect of water content on compressibility

The dredged slurry has a high water content (>70%)[19–20]. The in-situ water content of the dredged slurry collected from Taizhou is 78% after self-weight consolidation, close to two times its liquid limit (w_L). The one-dimensional consolidation tests were performed on the remolded slurry with a wide range of initial water contents from 70% (1.75 times w_L) to 140% (3.50 times w_L). Since the initial water content w_0 of the sample is greater than its liquid limit w_L, to prevent the sample from being squeezed out through the clearance gap between the ring and the upper porous stone during loading. Therefore, the standard oedometer apparatus was modified such that the initial vertical effective stress is low and suitable for the studied soil samples with high initial water contents[21]. The oedometer test adopted small increment multistage loading, and the loading sequence was 1.0, 2.0, 3.0, 4.0, 6.0, 8.0, 10.0, 12.5, 25.0, 50.0, 100.0, 200.0 and 400.0 kPa. The duration of every stress increment was 24 h.

The void ratio of soils with high initial water contents usually decreases rapidly due to the rapid drainage of the free pore water during consolidation. The compressibility of the soil with high initial water contentsvaries in a nonlinear fashion.. The nonlinear compression model of reconstituted soils is typically presented by the semi-logarithmic $e-\lg\sigma'$ model (e is the void ratio and σ' is the vertical effective stress). Butterfield[22] first proposed the bilogarithmic plot of $\lg(1+e)$ or $\ln(1+e)$ against $\lg\sigma'$ or to

$\ln\sigma'$ interpret the oedometer test data of undisturbed samples for soft natural clays. The compression curve can be better represented by two straight lines in the bilogarithmic plot of $\lg(1+e)-\lg\sigma'$ and $\ln(1+e)-\ln\sigma'$ than in the semi-logarithmic plot of $e-\lg\sigma'$, which is more reliable for the settlement and consolidation analysis for soft natural clays[23]. According to the studies by Onitsuka et al.[24], the linear relationship in the plot of $e-\lg\sigma'$ for the reconstituted soils can be alternatively represented by a linear relationship in the bilogarithmic plot $\lg(1+e)-\lg\sigma'$

The oedometer test data for the slurry at different initial water contents in the current study is interpreted in the bilogarithmic $\lg(1+e)-\lg\sigma'$ plot, as shown in Fig.2.

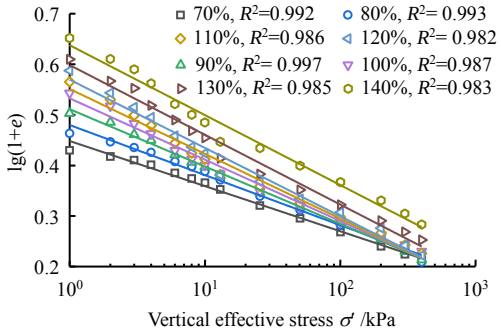

Fig. 2 Compression curves of Taizhou clay with different initial water contents

As shown in Fig. 2, the data of reconstitutedsoil with different initial water contents can be well represented by a linear relationship in the bilogarithmic $\lg(1+e)-\lg\sigma'$ plot. The following linear relationship between void ratio e and vertical effective stress σ' can be used to fit the oedometer test data for soils at eight different initial water contents:

$$\lg(1+e)=-C_{c1}\lg\sigma'+b_1 \qquad (1)$$

where $-C_{c1}$ and b_1 are the intercept and the gradient in the bilogarithmic $\lg(1+e)-\lg\sigma'$ plot, and C_{c1} is the modified compression index. The fitting results for the linear relationship in Eq. (1) for soils at different water contents are summarized in Table 2.

Table 2 Fitting parameters of the compression curves in slurry samples with different initial water contents

Initial water content w_0 /%	$-C_{c1}$	b_1	Correlation coefficient R^2
70	–0.089 19	0.448 44	0.992 00
80	–0.098 93	0.480 00	0.992 74
90	–0.113 32	0.511 35	0.997 37
100	–0.121 30	0.532 85	0.987 31
110	–0.128 16	0.551 32	0.986 24
120	–0.135 02	0.569 79	0.982 38
130	–0.137 86	0.598 55	0.984 89
140	–0.138 24	0.637 88	0.983 30

Hong et al.[21] conducted consolidation tests on remolded clays and studied the compression characteristics extending Burland's intrinsic compression curve concept[25]. They found that the compression curve could be well represented by two straight lines in the bilogarithmic $\lg(1+e)-\lg\sigma'$ plot, similar to the compression characteristics of natural sedimentary soils. Based on the similarity of compression curves between reconstituted clays and natural soils, Hong et al.[21] concluded that there should be a particular stress, which is referred as "suction pressure", that resists the load and results in low compressibility in the range of low stresses, similar to the consolidation yield stress for natural soils. The suction pressure of reconstituted clays can be determined in the same fashion as the consolidation yield stress for natural soils, which is the vertical effective stress corresponding to the intersection point of the two straight lines in the bilogarithmic $\lg(1+e)-\lg\sigma'$ plot for the oedometer test data. The initial water contents in the current study vary from 1.75 times its liquid limit to 3.50 times its liquid limit, which are relatively higher than that in Hong et al.[21] (i.e. from 0.7 times the liquid limit to 2.0 times the liquid limit of the studied clays). Therefore, the suction pressure that resists the load is lower than the first vertical stress applied. Consequently, the compression curves of Taizhou clay are represented by only one straight line, other than the bilinear lines in the bilogarithmic $\lg(1+e)-\lg\sigma'$ plot, as shown in Fig. 2. The initial vertical effective stresses are taken as the suction pressures that resist the load for the reconstituted Taizhou clays at high initial water contents. Based on the model in Eq. (1) and the fitting parameters summarized in Table 2, the initial vertical effective stress, σ'_0 can be evaluated with known initial void ratios for reconstituted Taizhou clays at different initial water contents (i.e. $e_0=w_0G_s$) as shown in Table 3.

Table 3 Initial effective stress of soil samples with different initial water contents

Initial water content w_0 /%	Initial vertical effective stress σ'_0 /kPa
70	0.877 76
80	0.676 41
90	0.687 03
100	0.587 45
110	0.439 39
120	0.400 44
130	0.419 32
140	0.316 22

The higher the initial water content w_0, the lower the corresponding initial vertical effective stress σ'_0, the greater the modified compression index, and the larger the soil compressibility, based on the results shown in Tables 2 and 3. Within a wide range of initial water contents (70% to 140%), the relationship between the initial vertical effective stress σ'_0 and the initial water content w_0 and the relationship between the modified compression index C_{c1} and the initial water content w_0 are determined based on test data and expressed by the following regressed equations with correlation coefficients R^2 of 0.950 and 0.992,

$$\sigma_0' = 252.0/(w_0^{1.333}) \quad (2)$$

$$C_{c1} = 0.151\,1 - 0.369\,7\exp(-w_0/39.70) \quad (3)$$

2.3 Effect of water content on permeability

The permeability coefficient is one of the key parameters for the theoretical solution of vacuum preloading. As shown in Fig. 3, the falling-head permeability test apparatus was used to determine the permeability coefficient of the reconstitued Taizhou clay (soft silty clay) at different initial water contents.

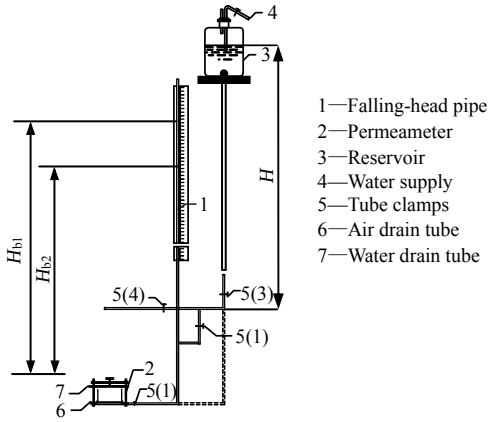

Fig. 3 Schematic diagram of the falling head permeability permeameter[18]

The anisotropy of the soil usually results in horizontal permeability coefficient $k_h >$ vertical permeability coefficient k_v during the vacuum preloading process. Due to a low clay-size fraction, the stress-induced anisotropy in Taizhou clay might be limited[26]. Therefore, it is assumed that $k_{h0} = 1.2k_{v0}$ in this study, where k_{h0} and k_{v0} are the initial horizontal and vertical permeability coefficients, respectively. The k_{h0} values of the remolded soil specimens are given in Table 4.

Table 4 Model parameters for consolidation calculation of slurry with different initial water contents

Reference	Initial water content w_0 /%	Parameters				
		P_0 /kPa	σ' /kPa	e_0	k_{h0} /(cm·s^{-1})	P_{ave}
This study	70	85	85.878	1.841	2.083×10^{-6}	2.875
	80	85	85.676	2.139	3.420×10^{-6}	2.329
	90	85	85.687	2.387	8.333×10^{-6}	1.590
	100	85	85.587	2.638	1.519×10^{-5}	1.333
	110	85	85.439	2.955	3.061×10^{-5}	1.156
	120	85	85.400	3.202	5.097×10^{-5}	1.002
	130	85	85.419	3.473	8.614×10^{-5}	0.949
	140	85	85.316	4.093	2.565×10^{-4}	0.940
Sun et al.[35]	N/A	85	86.336	3.676	1.944×10^{-7}	0.880
Yu[31]	100.100	85	85.626	2.610	1.560×10^{-5}	1.327

The consolidation of soils at high initial water contents occurs when subjected to vacuum preloading, which leads to the reduction in the void ratio and the coefficient of permeability[27]. Taylor[28] proposed the semi-logarithmic $e - \lg k_v$ plot to describe the variation of coefficient of permeability with the void ratio change, which has been validated for describing the nonlinear consolidation behavior of soils with high initial water contents via numerous experimental studies. The $e - \lg k_v$ model has been employed or modified by various researchers to investigate the nonlinear variation of the coefficient of permeability during the consolidation process. For example, Zeng et al.[29] provided the following regressed equation relating the vertical coefficient of permeability k_v to the void ratio e,

$$\lg(k_v) = -7.4 + 8.4\lg(1+e) - 7.2\lg(1+e_L) \quad (4)$$

where e_L is the void ratio of the soil at the liquid limit.

The comparison between the measured values of the vertical coefficient of permeability and the predicted values by Zeng's model is shown in Fig. 4. The good agreement (correlation coefficient = 0.965) between the measured and the predicted values indicates that Zeng's model is capable of modeling the variation of the coefficient of permeability with respect to the void ratio of the reconstituted soil. Thus, Zeng's model for predicting the coefficient of permeability is also used in this study.

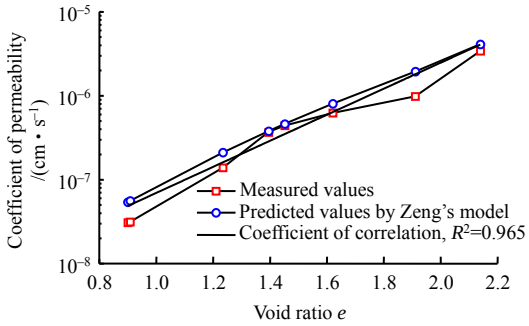

Fig. 4 Comparison between measured and predicted coefficient of permeability by Zeng's model

3 Analytical model development

3.1 Proposition of analytical model

The radial consolidation behavior of the dredged slurry is investigated using an axisymmetric model, following the analytical model for consolidation under vacuum preloading proposed by Perera et al.[30]. In the current study, the nonlinear variations of compressibility and permeability with respect to void ratio are predicted by the linear compression curve in the bilogarithmic $\lg(1+e) - \lg\sigma'$ plot and the linear equation between the coefficient of permeability and the void ratio in the bilogarithmic $\lg(1+e) - \lg k_v$ plot, respectively. The consolidation characteristic of the dredged slurry at high initial water contents is modelled, taking the "soil column" effect and the effect of the initial water content on the initial effective stress and the compressibility into consideration. The alteration of the compressibility and permeability of the dredged slurry at high initial water contents due to the drain installation, which is referred as "smear" effect, could be ignored[20, 31].

Zhou and Chai[32] established the consolidation model for the dredged slurry at high initial water content under vacuum preloading, considering the effect of non-uniform consolidation on the average degree of consolidation with the equivalent "smear" effect concept. Their study explained the discrepancy between the prediction by Hansbo's consolidation model of vertical drainage and the field observation and provided insight into the effect of non-uniform consolidation of slurry on PVD- induced consolidation. The dredged slurry flowed into the PVD, and a soil column formed surrounding the PVD, which resulted in the non-uniform PVD-induced consolidation. Therefore, three zones are identified in the current study, namely the PVD zone, the soil column zone, and the influence zone surrounding the soil column[20, 31, and 33].

The main assumptions made in this study are summarized below: (i) the soil is fully saturated and homogeneous; (ii) both the soil grain and water are incompressible; (iii) only water flow and consolidation in the radial direction are allowed for relatively long drains; (iv) the seepage follows Darcy's law, and drainage is not considered within the equivalent radius of the PVD; (v) the variation of permeability along the radial direction in the clogging zone is assumed to be linear at any time[31], and Zeng's model $\lg(1+e)-\lg k_{\mathrm{v}}$ [29] is used to describe the variation of permeability with respect to the void ratio during the consolidation under vacuum preloading; (vi) the loss of vacuum is not considered, i.e., the vacuum is assumed to be constant with the depth of the drain; (vii) Hansbo's consolidation model is used to consider the consolidation behavior in vacuum preloading at different initial water content based on the equivalent "smear" effect concept[32]. The axisymmetric consolidation calculation model and the constant vacuum pressure distribution are shown in Fig. 5(a). The variation of the permeability coefficient with the radius of the soil column is shown in Fig.5(b). In which, H is the thickness of the soil layer; r_{w}, r_{s}, and r_{e} are the equivalent radius of the vertical drain, the radius of the soil column, and the radius of the PVD influence area, respectively; r_{w} is determined by the $r_{\mathrm{w}}=(a+b)/4$ (Rixner et al.[34]), where a and b are the width and the thickness of the vertical drain; k_{w} and k_{h} are the permeability coefficient of the vertical drain and that of the soil surrounding the soil column, respectively, which is continuous at the location with the radial coordinate of $r=r_{\mathrm{w}}$ and $r=r_{\mathrm{s}}$; and x-axis and z-axis stand for the radial and the vertical coordinate, respectively.

The average degree of consolidation (U_{p}) of soils under vacuum preloading using the pore pressure distribution profiles can be written as

$$U_{\mathrm{p}}=\frac{\int_0^H\int_{r_{\mathrm{w}}}^{r_{\mathrm{s}}}2\pi(u_0-u_{\mathrm{s}})r\mathrm{d}r\mathrm{d}z+\int_0^H\int_{r_{\mathrm{s}}}^{r_{\mathrm{e}}}2\pi(u_0-u)r\mathrm{d}r\mathrm{d}z}{\int_0^H\int_{r_{\mathrm{w}}}^{r_{\mathrm{e}}}2\pi(u_0-u_\infty)r\mathrm{d}r\mathrm{d}z} \tag{5}$$

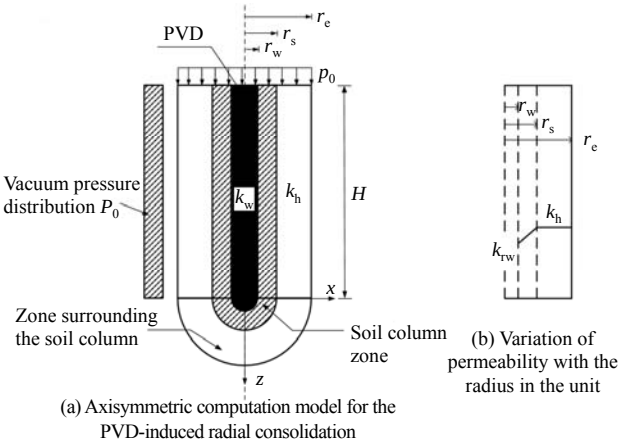

Fig. 5 Schematic illustration of the axisymmetric consolidation of the dredged slurry under vacuum preloading

where u is the pore water pressure at depth z in the zone outside the soil column at any given time; u_{s} is the pore water pressure at depth z in the soil column zone at any given time; u_0 is the initial pore water pressure; and u_∞ is the ultimate pore water pressure when the vacuum pressure applied for a relatively long duration.

Excess pore pressure ratio (R_{u}) can be defined as

$$R_{\mathrm{u}}=\frac{\overline{u}_{\mathrm{t}}}{\Delta\sigma'} \tag{6}$$

where $\Delta\sigma'$ is the preloading pressure applied, which equals the additional load (p_0) and the magnitude of vacuum pressure (P_0) and $\overline{u}_{\mathrm{t}}$ is the average excess pore pressure at any given time (t) in the unit. Combining with the definition of R_{u} in Eq. (6), Eq. (5) can be rearranged as

$$\left.\begin{aligned}\overline{u}_{\mathrm{t}}&=\frac{\int_0^H\int_{r_{\mathrm{w}}}^{r_{\mathrm{s}}}2\pi r u_{\mathrm{s}}\mathrm{d}r\mathrm{d}z+\int_0^H\int_{r_{\mathrm{s}}}^{r_{\mathrm{e}}}2\pi r u\mathrm{d}r\mathrm{d}z}{\pi(r_{\mathrm{e}}^2-r_{\mathrm{w}}^2)H}\\ U_{\mathrm{p}}&=1-(R_{\mathrm{u}}+\frac{P_0}{\Delta\sigma'})\end{aligned}\right\} \tag{7}$$

Integrating the expression of $\overline{u}_{\mathrm{t}}$, the expression of R_{u} in Eq. (6) can be rewritten as (details of derivation are given in appendix A)

$$R_{\mathrm{u}}=\left[\frac{p_0}{\Delta\sigma'}+\frac{(1+k_{\mathrm{l}})}{2}\frac{P_0}{\Delta\sigma'}\right]\exp\left(\frac{-8T_{\mathrm{h}}^*}{\mu}\right)-\frac{(1+k_{\mathrm{l}})}{2}\frac{P_0}{\Delta\sigma'} \tag{8}$$

where k_{l} is the attenuation coefficient of vacuum preloading, which is taken as unity in this study. The dimensionless parameter μ is expressed as

$$\mu=\ln\left(\frac{n}{s}\right)-\frac{3}{4}+\frac{\kappa(s-1)}{s-\kappa}\ln\left(\frac{s}{\kappa}\right) \tag{9}$$

where n is the ratio of $r_{\mathrm{e}}/r_{\mathrm{w}}$ and s is the ratio of $r_{\mathrm{s}}/r_{\mathrm{w}}$ and is taken as 3[20] in this study. The non-uniform consolidation phenomenon of the

dredged slurry at high initial water contents is typically ascribed to the "clogging effect" with the formation of a denser "soil column" that is induced by the more rapid consolidation for the soil surrounding the PVD. The "clogging effect" is usually considered in the consolidation model through the permeability coefficient ratio κ, which is the ratio of the horizontal permeability coefficient in the zone outside the soil column and the horizontal permeability coefficient at the boundary between the equivalent radius of PVD and the soil column (k_h / k_{rw}). Numerous previous studies argued that the ratio κ is constant[17, 20, and 32], which is taken as 300[20] in this study.

The corrected dimensionless time factor (T_h^*) in Eq. (8) is the correction for the dimensionless time factor (T_{h0}) and is expressed as

$$T_h^* = P_{ave} T_{h0} \tag{10}$$

$$P = \left(\frac{\sigma'}{\sigma'_0} \right)^{-C_{c1}A_2+1+C_{c1}} \tag{11}$$

where P is the function for the correction factor.

Thus, the correction factor (P_{ave}) can be evaluated by

$$P_{ave} = \frac{1}{2}\left[\left(\frac{\sigma'_0 + \Delta\sigma'}{\sigma'_0} \right)^{-C_{c1}A_2+1+C_{c1}} + 1 \right] \tag{12}$$

$$T_{h0} = \frac{c_{h0} t}{d_e^2} \tag{13}$$

$$c_{h0} = \frac{k_{h0}}{m_{v0}\gamma_w} \tag{14}$$

where A_2 is the model parameter associated with the term $\lg(1+e)$ in Eq. (4); c_{h0} is the radial coefficient of consolidation; t is the consolidation time; d_e is the diameter of the influence zone; m_{v0} is the initial coefficient of volumetric compressibility; and γ_w is the unit weight of water. The initial effective stress (σ'_0) and modified compression index (C_{c1}) are related to the initial water content, and the σ'_0 is estimated by Eq. (2). The corrected time factor (T_h^*) at any given time can be calculated based on Eqs. (10)–(14). Thus, the excess pore pressure ratio (R_u) can be evaluated by combing with other model parameters by Eq. (8). Therefore, the average degree of consolidation (U_p) at any given time can be determined by plugging the R_u into Eq. (7).

3.2 Validation of analytical model

The comparison among the analytical model proposed in this study, the model provided by Perera et al.[30], and this by Cai et al.[20] is shown in Fig. 6. In order to compare the proposed model to the results of Perera et al.[30], the model parameters are taken as $k_1 = 1$, $\sigma'_0 = 10$ kPa, $P_0 = 40$ kPa, $p_0 = 40$ kPa, $k_{h0} = 5.58 \times 10^{-8}$ cm/s, $C_c = 0.74$, and $C_k = 0.65$ in this study, consistent with Perera et al.[30]. In order to compare the proposed model to the studies by Cai et al.[20], the model parameters k_1, k_h / k_c, n, and s are taken as mentioned above, k_c is the coefficient of permeability in the soil column zone, and C_c / C_k = 0.50 and c_h =0.32 m^2/a are selected. As shown in Fig. 6, the analytical model of the average degree of consolidation is higher than that of Perera's model at the early stage of the consolidation because different compression models and permeability models are selected, and the "soil column" effect in the process of vacuum preloading of dredged sludge with high water content is considered in this study. The "soil column" effect is constant in this study, which is different from the model with the time-dependent "soil column" effect proposed by Cai et al.[20]. Therefore, the proposed analytical model has a higher degree of consolidation than that by Cai's model at the early stage of the consolidation, but it tends to be consistent with the consolidation. In summary, the similarity between the proposed analytical model and the predictions by two existing models (i.e., Perera's model and Cai's model) verifies the validity of the solution in this study.

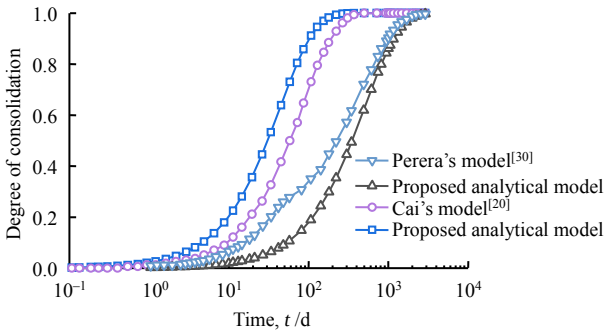

Fig. 6 Comparison between proposed solution and previous studies

4 Laboratory model test

In order to verify the accuracy of the above analytical solution of vacuum preloading, a set of laboratory model tests of vacuum preloading were carried out, and the test results were compared with the theoretical calculation values.

4.1 Experimental plan

The selection of soil samples and the range of initial water content were consistent with the improved one-dimensional consolidation test above. Eight groups of vacuum preloading laboratory model tests were carried out. The pore water pressure and surface settlement were monitored by sensors during the tests.

4.2 Experimental apparatus

As shown in Fig. 7(a), the laboratory test apparatus mainly consisted of three parts: (i) a model barrel; (ii) a vacuum supply and water drainage system; and (iii) a data-acquisition system (DAS). The model barrel was 500 mm in inner diameter and 600 mm in height. The barrel was sealed by the membrane with the help of flange clamps. The vacuum pump was connected to the model barrel through the vacuum pipes which

inserted the holes on the wall of the barrel, avoiding the loss of vacuum. The vacuum supply and water drainage system included the PVD, the air-water separation flask, and the vacuum pump. The PVD had a width of 100 mm, a thickness of 4 mm and a equivalent pore diameter of 75 μm. The air-water separation flask incorporating with the electronic balance were used to collect and weigh the drained water. The data-acquisition system consisted of mini pore water pressure sensors, a vacuum probe, and linear variable differential transformers (LVDTs). The pore water pressure sensors (P_1-P_3) and the vacuum probe (C_1) were installed near the PVD; the LVDTs were installed on the top of the sealing membrane (Fig. 7(a)). The photo of the experimental apparatus is shown in Fig. 7(b).

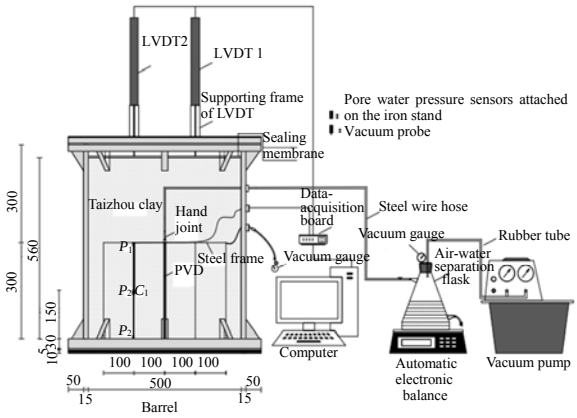

(a) Diagram of the experimental setup (unit: mm)

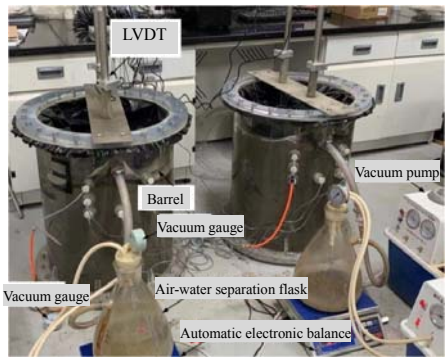

(b) Physical photo of the experimental setup

Fig. 7 Experimental setup: (a) diagram; (b) photo

4.3 Experimental procedures

The experimental procedures are as follows: (i) the PVD, the pore water pressure sensors, and the vacuum probe were installed and fixed in the model barrel by the steel frame, as shown in Fig. 7(a); (ii) the slurry with high initial water content was filled into the barrel and reached the initial height of 560 mm; (iii) the barrel was sealed immediately after filling the slurry, and two LVDTs were installed on the top surface of the sealing membrane; (iv) the vacuum pump was connected to the air-water separation flask, which was connected to the barrel; the test was started with the stable vacuum pressure of 85 kPa (i.e., –85 kPa relative to atmospheric pressure) supplied by the vacuum pump; and (v) the measurements were obtained and stored by the data-acquisition system during the test, and the test was stopped after 60 d (1440 h).

5 Model test results and model validation

The measured average pore pressures varied with time during the model tests on slurries with eight different initial water contents are shown in Fig. 8. It indicates that the initial water content influences the transmission of vacuum pressure in the slurry. The variation rate of the pore pressure in the slurry decreases as the initial water content increases. After applying the vacuum pressure for 6 d, the pore water pressure decreases to –75 kPa relative to the atmospheric pressure in the slurry with the initial water content of 70%; on the other hand, that decreases to –32 kPa in the slurry with the initial water content of 140%. Therefore, the vacuum pressure applied may transmit more effectively in the slurry with a lower initial water content.

The average degree of consolidation can be given based on the measured average pore pressure (Fig. 8) as follows:

$$U'_{\mathrm{p}}=\frac{\overline{u}'_{\mathrm{t}}-\overline{u}'_0}{\overline{u}'_{\infty}} \tag{15}$$

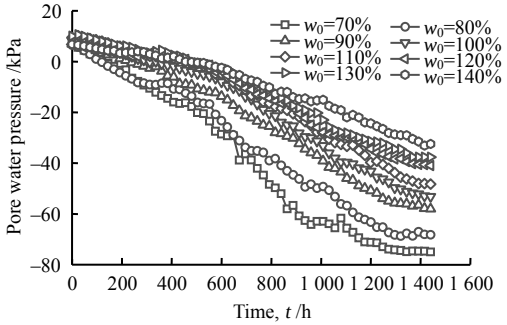

Fig. 8 Variation of average pore water pressure with time in dredged slurry with different initial water contents

where $\overline{u}'_{\mathrm{t}}$ is the measured average pore water pressure at any given time; $\overline{u}'_0$ is the measured initial average pore water pressure; and $\overline{u}'_{\infty}$ is the expected ultimate average pore water pressure under the vacuum pressure applied. The model parameters are given in Table 4 for estimating the average degree of consolidation based on the proposed analytical model. The related parameters derived from previous studies[31, 35] are also given in Table to validate the pore water pressure and settlement predictions by the proposed analytical model.

The ratios of pore water pressure-based average degree of consolidations predicted by the proposed analytical model (U_{p}) to those estimated by measured average pore water pressure by the laboratory model tests (U'_{p}) versus time are plotted in Fig. 9 for slurries with eight different initial water contents. The results obtained by previous studies, i.e. Sun et al.[31] and Yu[35], are included in Fig. 9 as well. The fluctuation of

the curves in Fig. 9 is due to the fluctuation in pore water pressure when the vacuum pump is replaced. The discrepancies exist between the results by the proposed model and those estimated by the measured pore water pressure, especially for the slurries with high initial water contents of 110%–140%. In fact, the predicted degree of consolidation by the proposed model are the average values over the entire slurry specimen, while the pore water pressures are measured by the pore water pressure sensors at three specific locations based on which the degree of consolidation are estimated. The measured results of the coefficient of permeability listed in Table 4 indicate that the permeability increases remarkably as the initial water content increases. In the proposed analytical model, the higher the initial water content of the slurry, the faster the average pore water pressure dissipates. The pore water pressure sensors are fixed on the iron stand in one column at different depths (Fig. 7(a)), which measure the pore water pressures at the specific locations in the slurry with an initial height of 560 mm. This results in the discrepancies between the predicted average pore water pressure and measured pore water pressures, and consequently the discrepancies between the predicted values and measured values of the average degree of consolidations as shown in Fig. 9.

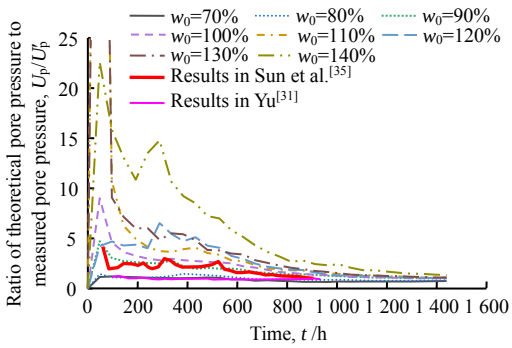

Fig. 9 Plots of the ratio of the theoretical pore pressure-based degrees of consolidation to the measured values by the current study and the previous studies versus time

The measured settlements on the top surface of the slurries with different initial water contents during the model tests are shown in Fig. 10. Thus, the settlement-based degree of consolidation can be estimated as

$$U'_s = \frac{\overline{S}'_t}{\overline{S}'_\infty} \tag{16}$$

where $\overline{S}'_t$ is the measured average settlement of soil top surface at any given time and $\overline{S}'_\infty$ is the expected ultimate average settlement under the vacuum pressure applied.

The settlement at any given time and the ultimate settlement can be predicted for slurries with different initial water contents by Table 2 and Eqs. (A25) and (A26) in the Appendix A. Thus, the settlement-based average degree of consolidation can be estimated by Eq.(16). Fig. 11 presents the plots of the ratio of predicted values to measured values of the settlement-based degree of consolidation versus time for slurries with different initial water contents. The results obtained by previous studies, i.e. Sun et al.[31] and Yu[35], are also included in Fig. 11. It can be found that the predicted values are higher than the measured values for the slurries with a relatively low range of initial water contents (i.e. 70%–90%), when the duration of the consolidation is shorter than 200 h. In fact, the lower the initial water content, the lower initial coefficient of permeability the slurry has. The pore water drained through the PVD once the vacuum pressure applies. The slurries with lower initial water contents settle slowly at the early stage of the consolidation, which results in a lower measured settlement than that predicted by the proposed model. As the consolidation continues, the predicted values agree well with the measured values and the ratios of the predictions to the measurements converge to unity. It indicates that the proposed analytical model can well predict the consolidation characteristics of slurries with high initial water contents.

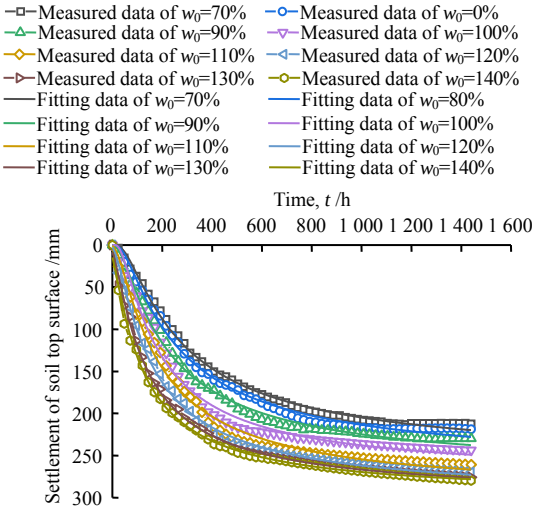

Fig. 10 Variations of measured and fitted average settlements versus time

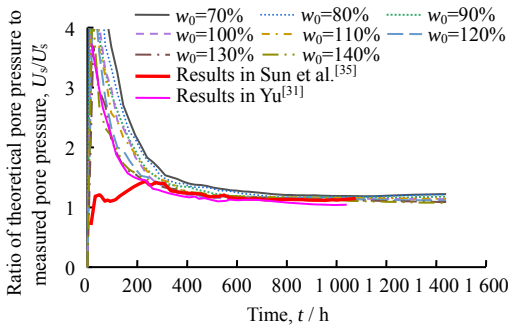

Fig. 11 Plots of the ratio of the theoretical settlement-based degrees of consolidation to the measured values by the current study and the previous studies versus time

Based on the comparisons in Figs. 9 and 11, the predicted settlement-based degree of consolidation agrees better than the predicted pore water pressure-

based degree of consolidation with the measured value. The pore water pressure sensors can only indicate the dissipation of pore water pressure at the monitoring points; while the prediction by the proposed analytical model reflects the average dissipation of pore water pressure over the entire slurry in the model barrel. Thus, the accuracy of the measured pore water pressure-based degree of consolidation is limited by the location and number of the monitoring points. On the other hand, the influence of the monitoring points on the settlement measurements on the top surface of the slurry is rather limited. Therefore, the differences between predicted settlement-based degrees of consolidation and the measured values are relatively small. Moreover, the comparisons between the predictions with the model parameters for other types of soils listed in Table 4 and the results by previous studies[31, 35] also indicate the good performance of the proposed analytical model, as shown in Figs. 9 and 11.

6 The specific procedures for predicting the consolidation behavior of dredged slurries

The characteristics of reconstituted clays are intrinsic properties, which are totallydifferent from thosenatural deposited clays. Thus, the compressibility and strength characteristics of reconstituted clays can be used to explain the properties of natural deposited clays. The following procedures are recommended to predict the consolidation behavior of various types of dredged slurries under vacuum preloading:

(i) The compression indexes of the soil are determined by the compression curve based on the oedometer test results. The initial effective stress can be calculated by Eq. (2), combining with associated parameters.

(ii) The initial permeability coefficient of the dredged slurry is determined by the permeability test. Subsequently, the relationship between the permeability and the void ratio can be derived from the compression curve.

(iii) The theoretical degree of consolidation based on the settlement of dredged slurries with different initial water contents under vacuum preloading can be estimated by Eqs. (4)–(16) and Eq.s (A17)–(A26) in appendix A, considering the nonlinearity of compressibility and permeability in the vacuum preloading process.

(iv) The proposed analytical model is validated by comparing the predicted degree of consolidation with the measured value.

7 Conclusions

(i) The oedometer test results on slurries with different initial water contents indicate that the initial effective stress (σ_0') decreases in a negative power function fashion as the initial water content (w_0) increases and the modified compression index (C_{c1}) increases in an exponential function fashion.

(ii) The impact of the initial water content on the dissipation of pore water pressure and settlement behavior of the slurry has been investigated by laboratory model tests of PVD-induced consolidation under vacuum preloading. It can be found that the dredged slurry with a higher water content settles less, and the pore water pressure dissipates more slowly.

(iii) The analytical model is established for predicting the consolidation behavior under vacuum preloading considering the nonlinearity of the compressibility and permeability for dredged slurries with different initial water contents. The comparisons between the predictions and measurements indicate that the proposed model works well, especially for the slurries with high initial water contents.

References

[1] CHEN Xiang-long, JIANG Shun-wu, JIN Ya-wei, et al. Amendment of vacuum preloading technique in the application at Hainan Sea Flower Island and its improvement mechanism[J]. Civil Architectural and Environmental Engineering, 2017, 39(2): 75–83.

[2] RUJIKIATKAMJORN C, INDRARATNA B. Analytical solution for radial consolidation considering soil structure characteristics[J]. Canadian Geotechnical Journal, 2014, 52(7): 947–960.

[3] WANG Dong-xing, TANG Yi-kai, WU Lin-feng. Evaluation on deep dewatering performance of dredged sludge treated by chemical flocculation-vacuum preloading[J]. Rock and Soil Mechanics, 2020, 41(12): 3929–3938.

[4] DENG Yue-bao. Analytical theory and finite element analysis for consolidation of soft soils by vertical drains[D]. Hangzhou: Zhejiang University, 2013.

[5] CHEN Jun-sheng, MO Hai-hong, LI Jin-hua. Amendments consolidation theory of vertical sand drains considering drainage board clogging in vacuum preloading[J]. Port & Waterway Engineering, 2017, 526(3): 150–156, 168.

[6] CAI Y Q, WANG J, MA J, et al. A new method to improve the effectiveness of vacuum preloading on the consolidation of dredged fill in Wenzhou[J]. Japanese Geotechnical Society Special Publication, 2016, 2(51): 1794–1797.

[7] CAI Y Q, QIAO H H, WANG J, et al. Experimental tests on effect of deformed prefabricated vertical drains in dredged soil on consolidation via vacuum preloading[J]. Engineering Geology, 2017, 222: 10–19.

[8] CHAI J C, CARTER J P, HAYASHI S. Ground deformation induced by vacuum consolidation[J]. Journal of Geotechnical & Geoenvironmental Engineering, 2005, 131(12): 1552–1561.

[9] LI Jing-hua. Experimental study on clogging behavior of PVD in Nansha soft clay improved by vacuum preloading[D]. Guangzhou: South China University of Technology,

2015.

[10] PU He-fu, PAN You-fu, KHOTEJA D, et al. Model test on dewatering of high-water-content dredged slurry by flocculation-horizontal vacuum two-staged method[J]. Rock and Soil Mechanics, 2020, 41(5): 1502–1509.

[11] SHEN Jie. Laboratory model test of vacuum preloading on dredged clays at high initial water contents[D]. Nanjing: Southeast University, 2015.

[12] YAN S W, CHU J. Soil improvement for a storage yard using the combined vacuum and fill preloading method[J]. Canadian Geotechnical Journal, 2005, 42(4): 1094–1104.

[13] LOU Chen-hui. Experimental study on the effect of PVD and initial water content on vacuum preloading reinforcement and range of drainage dredged fill[D]. Wenzhou: Wenzhou University, 2019.

[14] DENG Y F, LIU L, CUI Y J, et al. Colloid effect on clogging mechanism of hydraulic reclamation mud improved by vacuum preloading[J]. Canadian Geotechnical Journal, 2018, 56(5): 611–620.

[15] WANG P, HAN Y, ZHOU Y, et al. Apparent clogging effect in vacuum-induced consolidation of dredged soil with prefabricated vertical drains[J]. Geotextiles and Geomembranes, 2020, 48(4): 524-531.

[16] HAN Yan-bing. Lateral movement of soil between PVDs during consolidation of dredged silt under vacuum preloading[D]. Wenzhou: Wenzhou University, 2019.

[17] TAI P, INDRARATNA B, RUJIKIATKAMJORN C. Experimental simulation and mathematical modelling of clogging in stone column[J]. Canadian Geotechnical Journal, 2017, 55(3): 427–436.

[18] State Administration of Quality and Technical Supervision. GB/T 5012 — 2019 Standard for geotechnical testing method[S]. Beijing: China Planning Press, 2019.

[19] PAN Xiao-dong, ZHOU Lian-mo, SUN Hong-lei, et al. Vacuum preloading test for high moisture content slurry using particle image velocimetry[J]. Journal of Zhejiang University (Engineering Science), 2020, 54(6): 1078–1085.

[20] CAI Yuan-qiang, ZHOU Yue-fu, WANG Peng, et al. Calculation on settlement of dredged slurry treated by vacuum preloading method with consideration of clogging effects[J]. Rock and Soil Mechanics, 2020, 41(11): 3705–3713.

[21] HONG Z S, YIN J, CUI Y J. Compression behaviour of reconstituted soils at high initial water contents[J]. Géotechnique, 2010, 60(9): 691–700.

[22] BUTTERFIELD R. A natural compression law for soils (an advance on *e*-log*p*′)[J]. Géotechnique, 1979, 29(4), 469–480.

[23] SRIDHARAN A, PRAKASH K. Discussion on 'interpretation of oedometer test data for natural clays'[J]. Soils and Foundations, 1996, 36(3): 146–148.

[24] ONITSUKA K, HONG Z S, HARA Y, et al. Interpretation of oedometer test data for natural clays[J]. Journal of the Japanese Geotechnical Society, 1995, 35(3): 61–70.

[25] BURLAND J B, ENG F. On the compressibility and shear strength of natural clays[J]. Géotechnique, 1990, 40(3): 329–378.

[26] CHAI J C, JIA R, NIE J X, et al. 1D deformation induced permeability and microstructural anisotropy of Ariake clays[J]. Geomechanics & Engineering, 2015, 8(1): 81–95.

[27] TAVENAS F A, JEAN P, LEBLOND P, et al. The permeability of natural soft clays. part II: permeability characteristics[J]. Canadian Geotechnical Journal, 1983, 20(4): 645–660.

[28] TAYLOR D W. Fundamentals of soil mechanics[J]. Soil Science, 1948, 66(2): 161.

[29] ZENG L L, CAI Y Q, CUI Y J, et al. Hydraulic conductivity of reconstituted clays based on intrinsic compression[J]. Géotechnique, 2020, 70(3): 268–275.

[30] PERERA D, INDRARATNA B, LEROUEIL S, et al. Analytical model for vacuum consolidation incorporating soil disturbance caused by mandrel-driven drains[J]. Canadian Geotechnical Journal, 2016, 54(4): 547-560.

[31] YU Fan. Soil plugging effect of PVD consolidation in high water flow mud under vacuum pressure[D]. Wenzhou: Wenzhou University, 2018.

[32] ZHOU Y, CHAI J C. Equivalent 'smear' effect due to non-uniform consolidation surrounding a PVD[J]. Géotechnique, 2017, 67(5): 410–419.

[33] LIU S J, CAI Y Q, SUN H L, et al. Consolidation considering clogging effect under uneven strain assumption[J]. International Journal of Geomechanics, 2021, 21(1): 1–12.

[34] RIXNER J J, KRAEMER S R, SMITH A D. Prefabricated vertical drains. Vols. I, II and III[R]. Washington, D.C.: [s. n.], 1986.

[35] SUN H L, WENG Z Q, LIU S J, et al. Compression and consolidation behaviors of lime-treated dredging slurry under vacuum pressure[J]. Engineering Geology, 2020, 270: 1–10.

Appendix A

Following the analytical model for vacuum consolidation proposed by Perera et al.[30], the average excess pore water pressure $\overline{u}_t$ at any given time t in

the unit can be given as

$$\overline{u}_{\mathrm{t}}=\frac{\partial \varepsilon}{\partial t}\frac{r_{\mathrm{e}}^{2}\mu}{2k_{\mathrm{h}}}\gamma_{\mathrm{w}}-\frac{(1+k_{1})}{2}P_{0} \tag{A1}$$

Excess pore water pressure ratio R_{u} is defined as

$$R_{\mathrm{u}}=\frac{\overline{u}_{\mathrm{t}}}{\Delta\sigma'} \tag{A2}$$

Substituting Eq. (A1) into Eq. (A2), the excess pore water pressure ratio can be expressed as

$$R_{\mathrm{u}}=\frac{\partial e}{\partial\sigma'}\frac{\partial(\sigma-\overline{u}_{\mathrm{t}})}{\partial t}\frac{(2r_{\mathrm{e}})^{2}\mu}{8k_{\mathrm{h}}(1+e_{0})\Delta\sigma'}\gamma_{\mathrm{w}}-\frac{(1+k_{1})}{2}\frac{P_{0}}{\Delta\sigma'} \tag{A3}$$

An instantaneous additional load p_0 and vacuum preloading P_0 are assumed, and it is assumed that these loads do not vary with time. Therefore, the total stress σ applied is constant and $\Delta\sigma'$ is the sum of additional load p_0 and vacuum preloading P_0. Thus, Eq. (A3) can be rewritten as

$$R_{\mathrm{u}}=-\frac{\partial e}{\partial\sigma'}\frac{\partial(\overline{u}_{\mathrm{t}})}{\partial t}\frac{(2r_{\mathrm{e}})^{2}\mu}{8k_{\mathrm{h}}(1+e_{0})\Delta\sigma'}\gamma_{\mathrm{w}}-\frac{(1+k_{1})}{2}\frac{P_{0}}{\Delta\sigma'} \tag{A4}$$

Based on Eq. (A2), find the partial derivative of R_{u} with respect to time t,

$$\frac{\partial R_{\mathrm{u}}}{\partial t}=\frac{1}{\Delta\sigma'}\frac{\partial\overline{u}_{\mathrm{t}}}{\partial t} \tag{A5}$$

The Eq. (A5) is transformed to obtain

$$\frac{\partial\overline{u}_{\mathrm{t}}}{\partial t}=\Delta\sigma'\frac{\partial R_{\mathrm{u}}}{\partial t} \tag{A6}$$

According to Eqs. (A4)–(A6), Eq. (A7) can be ob tained

$$\frac{\partial R_{\mathrm{u}}}{\partial t}=-\left[R_{\mathrm{u}}+\frac{(1+k_{1})}{2}\frac{P_{0}}{\Delta\sigma'}\right]\frac{(1+e_{0})}{\partial e/\partial\sigma'}\frac{2k_{\mathrm{h}}}{\mu r_{\mathrm{e}}^{2}\gamma_{\mathrm{w}}} \tag{A7}$$

Convert the partial derivative of R_{u} with respect to time t in Eq. (A7) to the partial derivative of R_{u} with respect to dimensionless time factor T_{h0} (the expression of T_{h0} is shown in Eq. (13) in the paper) to obtain Eq. (A8),

$$\frac{\partial R_{\mathrm{u}}}{\partial T_{\mathrm{h0}}}=\frac{\partial R_{\mathrm{u}}}{\partial t}\Big/\frac{\partial T_{\mathrm{h0}}}{\partial t}=-\frac{8}{\mu}\frac{m_{\mathrm{v0}}}{m_{\mathrm{v}}}\frac{k_{\mathrm{h}}}{k_{\mathrm{h0}}}\left[R_{\mathrm{u}}+\frac{(1+k_{1})}{2}\frac{P_{0}}{\Delta\sigma'}\right] \tag{A8}$$

The function P is defined by

$$P=\frac{m_{\mathrm{v0}}}{m_{\mathrm{v}}}\frac{k_{\mathrm{h}}}{k_{\mathrm{h0}}} \tag{A9}$$

Substituting Eq. (A9) into Eq. (A8) gives

$$\frac{\partial R_{\mathrm{u}}}{\partial T_{\mathrm{h0}}}=-\frac{8}{\mu}P\left[R_{\mathrm{u}}+\frac{(1+k_{1})}{2}\frac{P_{0}}{\Delta\sigma'}\right] \tag{A10}$$

Based on Eq. (1) in the paper, the following expressions for m_{v0} and m_{v} can be derived,

$$\left.\begin{aligned}m_{\mathrm{v0}}&=\frac{(-\mathrm{d}e/\mathrm{d}\sigma')_{\mathrm{t=0}}}{1+e_{0}}=\frac{10^{b_{1}}C_{\mathrm{c}_{1}}\sigma_{0}'^{\,-C_{\mathrm{c}_{1}}-1}}{1+e_{0}}\\ m_{\mathrm{v}}&=\frac{(-\mathrm{d}e/\mathrm{d}\sigma')}{1+e_{0}}=\frac{10^{b_{1}}C_{\mathrm{c}_{1}}\sigma'^{\,-C_{\mathrm{c}_{1}}-1}}{1+e_{0}}\end{aligned}\right\} \tag{A11}$$

$$\frac{m_{\mathrm{v0}}}{m_{\mathrm{v}}}=\left(\frac{\sigma_{0}'}{\sigma'}\right)^{-C_{\mathrm{c}_{1}}-1} \tag{A12}$$

Equation (4) describes the relationship between the vertical permeability coefficient and the void ratio. Therefore, the ratio of permeability coefficient on the right side of Eq. (A9) can be converted into

$$\frac{k_{\mathrm{h}}}{k_{\mathrm{h0}}}=(\frac{\sigma'}{\sigma_{0}'})^{-C_{\mathrm{c}_{1}}A_{2}} \tag{A13}$$

where A_2 is the coefficient with the term $\lg(1+e)$ in Eq. (4).

Substituting Eqs. (A12) and (A13) into Eq. (A9), the function P can be expressed as

$$P=\left(\frac{\sigma'}{\sigma_{0}'}\right)^{-C_{\mathrm{c}_{1}}A_{2}+1+C_{\mathrm{c}_{1}}} \tag{A14}$$

The above equation describes the radial consolidation of vertical drains with vacuum preloading under an instantaneous surcharge and vacuum, where, where the value of effective stress σ' varies from σ_0' to $\sigma_0'+\Delta\sigma'$. To simplify the partial differential equation (Eq. (A10)), the P value is taken as the average in the consolidation process and is given by

$$P_{\mathrm{ave}}=\frac{1}{2}\left[\left(\frac{\sigma_{0}'+\Delta\sigma'}{\sigma_{0}'}\right)^{-C_{\mathrm{c}_{1}}A_{2}+1+C_{\mathrm{c}_{1}}}+1\right] \tag{A15}$$

According to Eqs. (A9), (A10), (A14), and (A15), Eq. (A16) can be obtained:

$$\frac{\partial R_{\mathrm{u}}}{\partial T_{\mathrm{h}}^{*}}=-\frac{8}{\mu}\left[R_{\mathrm{u}}+\frac{(1+k_{1})}{2}\frac{P_{0}}{\Delta\sigma'}\right] \tag{A16}$$

The above equation is the first-order partial differential equation of R_{u}. Applying the conditions including (i) $R_{\mathrm{u}}\left(t=0\right)=p_{0}/\Delta\sigma'$ and (ii) $R_{\mathrm{u}}\left(t=t_{f}\right)=-P_{0}/\Delta\sigma'$. By integrating Eq. (A16) with respect to the corrected dimensionless time factor T_h^*, the value of R_{u} can be derived as follows:

$$R_{\mathrm{u}}=\left[\frac{p_{0}}{\Delta\sigma'}+\frac{(1+k_{1})}{2}\frac{P_{0}}{\Delta\sigma'}\right]\exp\left(\frac{-8T_{\mathrm{h}}^{*}}{\mu}\right)-\frac{(1+k_{1})}{2}\frac{P_{0}}{\Delta\sigma'} \tag{A17}$$

The corrected dimensionless time factor T_{h}^{*} in Eq. (A17) is defined as

$$T_{\mathrm{h}}^{*}=\frac{1}{2}\left[\left(\frac{\sigma_{0}'+\Delta\sigma'}{\sigma_{0}'}\right)^{-C_{\mathrm{c}_{1}}A_{2}+1+C_{\mathrm{c}_{1}}}+1\right]T_{\mathrm{h0}} \tag{A18}$$

Plugging the model parameters into Equation (A18), the value of T_{h}^{*} can be calculated. Substituting

the value of T_h^* into Eq. (A17), the value of R_u can be derived. Thus, the excess pore water pressure-based average degree of consolidation, U_p can be evaluated by substituting the value of R_u into Eq. (7).

Taking the effect of the initial water content w_0 on the initial effective stress σ_0' and the modified compression index C_{c1} into consideration, the excess pore water pressure ratio expression in Eq. (A17) can be rewritten as

$$R_u = \lambda_1 \exp\left(\frac{4}{\mu} \frac{\left[(1+\frac{\Delta\sigma'}{\lambda_{w1}})^{1-(1-A_2)\lambda_{w2}} + 1 \right] \lambda_{w1}^{(\lambda_{w2}-1)} \lambda_{w3}}{10^{b1} \gamma_w d_e^{\,2} \lambda_{w2}} \right) - \lambda_2 \tag{A19}$$

$$\lambda_1 = \frac{p_0}{\Delta\sigma'} + \frac{(1+k_1)}{2} \frac{P_0}{\Delta\sigma'} \tag{A20}$$

$$\lambda_2 = \frac{(1+k_1)P_0}{2\Delta\sigma'} \tag{A21}$$

$$\lambda_{w1} = C_1 / w_0^{\,d_1} \tag{A22}$$

$$\lambda_{w2} = C_2 \exp\left(-w_0/d_2\right) - C_3 \tag{A23}$$

$$\lambda_{w3} = G_s(1+w_0)(\rho_w/\rho_0)k_{h0}t \tag{A24}$$

where C_1, C_2, C_3, d_1, and d_2 are model parameters. With the derived value of R_u and the known total stress applied ($\Delta\sigma'$), the average excess pore water pressure at any give time, $\bar{u}_t$ can be calculated based on Eq.(A2). Combining the value of $\bar{u}_t$ and the initial effective stress (σ_0'), the effective stress (σ') at any time t can be obtained. Therefore, the void ratio (e) and the settlement (S_t) can be derived by the following equations:

$$\lg(1+e) = -C_{c1} \lg \sigma' + b_1 \tag{A25}$$

$$S_t = \frac{e_0 - e}{1+e_0} H \tag{A26}$$